Journal of Sailing Technology 2023, volume 8, issue 1, pp. 200-217.
The Society of Naval Architects and Marine Engineers.

Weather Routing Benefit for Different Wind Propulsion Systems

Maxime Dupuy
LIX, Ecole Polytechnique, D-ICE Engineering, France, maxime.dupuy@dice-engineering.com.

Lucas Letournel
D-ICE Engineering, France.

Ville Paakkari
NORSEPOWER, Finland.

François Rongère
D-ICE Engineering, France.

Severi Sarsila
NORSEPOWER, Finland.

Louis Vuillermoz
D-ICE Engineering, France.

Manuscript received August 8, 2023; revision received October 20, 2023; accepted November 25, 2023.

Abstract. Impact of weather routing on a post-panamax bulk carrier equipped with different wind propulsion systems was studied. The studied wind propulsion systems were rotor sails, wing sails, and suction wings and the studied route was a typical bulk carrier route between China and Brazil. A 4 degrees of freedom (4-DoF) performance prediction program was used to generate a performance model of the ship with different wind propulsion devices and the performance models were used in the voyage optimization. The voyage optimization simulations were carried out using historical weather data during the years 2015 to 2019 with one departure per week on both ways. It was found that there is a significant reduction in fuel consumption when weather routing is used on wind propulsion ships, but the magnitudes of the weather routing benefit vary from system to system depending on its versatility. Higher benefits from weather routing were found first for rotor sails, then for suction wings, and finally for wing sails.

Keywords: Wind Propulsion; Voyage Optimization; Weather Routing.

NOMENCLATURE

A	Cross sectional area of the suction wing's suction mesh [m^2]
c	Chord of the suction aerofoil [m]
C_q	Suction coefficient for suction wing [-]
F	Fuel consumption of the vessel [t]
H_S	Significant Waves Height [m]
P_e	Electric consumption of a wind propulsion system [kW]
Q	Volumetric flow rate [m^3/s]
T	Wind propulsion thrust [kN]
u	Vessel speed [m/s]
U_i	Freestream velocity [m/s]

U_s	Suction velocity [m/s]
W_A	Waves relative angle [°]
W_B	Weather routing benefit [%]
Z_m	height from base aerofoil [m]
β	Wing sail flap angle [°]
ΔF	Fuel saving [t]
ΔP	Main engine equivalent power [kW]
η_D	Total propulsive efficiency of a ship [-]
η_e	Electric efficiency of the suction wing [-]
λ	Ship's longitude [°]
ρ	Air density [kg/m^3]
ϕ	Ship's latitude [°]
4-DoF	4-Degree of Freedom
ETA	Estimated Time of Arrival
GCR - CS	Great circle route and constant speed routing scenario
MCR	Maximum Continuous Rating
OR - OS	Optimised route and optimized speed routing scenario
PPP	Performance Prediction Program
STW	Speed Through Water
TWA	True Wind Angle
TWS	True Wind Speed
WASP	Wind Assisted Ship Propulsion

1 INTRODUCTION

Wind propulsion is gaining momentum as a means to support the decarbonization of commercial shipping. As a source of primary renewable energy, wind propulsion technologies are highly dependent on the prevailing wind conditions. Recent studies (Mason, 2021, Paakkari et al., 2022, Dupuy, M., D. Dudka, L. Letournel, F. Rongere, and G. Vincke, 2023) have highlighted the importance of weather routing for the performance of wind propulsion as it has been shown that the performance of wind propulsion can be as much as doubled when weather routing is utilized. On the other hand, different wind propulsion technologies have significantly different characteristics in terms of propulsion performance. Comparisons between different wind propulsion systems have been made (Sarsila, 2022), but there is little publicly available research on the qualitative and quantitative differences between the various sail technologies with a weather routing focus.

Different wind propulsion technologies have distinct performance characteristics. These differences will be elaborated further later but generally speaking, some devices have their performance potential more ”evenly spread” along the points of sail (up-wind, beam-reach, broad-reach) while some other devices have more distinct areas of high performance and lower performance. This raises an interesting question of how these differences are reflected in operation when weather routing is applied. After all, weather routing is the art of adjusting the sail to the most economical operation point. This study compares the fuel-saving potential of different wind propulsion systems installed on a Post-Panamax bulk carrier using weather routing. The selected wind propulsion systems for this study are rotor sails, wing sails, and suction wings since these sail types are representative of the majority of commercially available wind propulsion technologies for ships. The purpose of this study is to understand the differences between different sail technologies by comparing and analyzing three different sail technologies when weather routing is deployed. The main objective is to compare the weather routing benefit of different wind propulsion systems, defining weather routing benefit as the increased wind propulsion fuel savings due to weather routing. It should be mentioned, that the purpose of this study is not to

compare the overall savings performance of different technologies but to focus on their qualitative and quantitative responses to weather routing. To achieve this, the different sail systems were sized so that the baseline performance on the route mean wind conditions was comparable between different systems.

Research has shown that hydrodynamic effects like drifting and increased rudder angles can decrease the power savings of wind propulsion systems. The impact of these effects is increased as the proportion of the wind power increases, and since the proportion of wind power on the studied ship was reasonably high, the interaction effects were accounted for by using a 4-Degree of Freedom (4-DoF) performance prediction program (PPP) in steady-state conditions. Also, the aerodynamic interaction effects can have an impact on the performance of the wind propulsion systems as the ship's hull and the other wind propulsion devices alter the flow field, but these effects were neglected in this study.

Limitations of this study are inherent in the models precision used for the Wind Assisted Ship Propulsion (WASP) performance evaluation. While generic empirical formulation were used for the ship models, ship data precision is of no matter here, since the ship is just a support for the comparison of the wind propellers. The precision on the wind propellers data is however predominant for this study and several approximations were considered. No interactions between units and between the ship and units were taken into account. Pre-trimmed load sails tables were also used as inputs for the PPP, which integrates a depowering process, via the application of a reduction coefficient on all loads, but not on the active power (see 2.1.2).

2 STUDY

2.1 Method

As mentioned in the introduction, the objective of this study is to compare weather routing strategies while considering 3 different sails technologies. To do so, we launched a large set of voyage optimization computations on a specific route, with operational constraints (such as Estimated Time of Arrival, or ETA, and weather limits) to have realistic results. For this study, the optimization aims at reducing the consumption while keeping the voyage duration constant.

For each departure date and the 4 ships (the conventional one and the 3 hybrid ships equipped with the different wind propulsion systems), we launch the following 2 scenarios of weather routing:

- GCR - CS: Great Circle Route and Constant Speed
- OR - OS: Optimised Route and Optimised Speed

From these computations, we analyzed each wind propulsion system's global results, to understand the behavior of the optimization process and its adaptability.

2.1.1 System scaling

To have a similar baseline performance for each system, the systems were scaled to have the same area of net savings (under the main engine equivalent power curve) in 13 kn vessel speed and 12.5 kn true wind speed. The vessel and wind speed were selected to correspond with the average operational profile and wind conditions on the studied route. The authors decided not to show the corresponding sizes of each system as the purpose of the paper is to focus on the impact on weather routing strategy and not to compare the performances.

The main engine equivalent power ΔP is defined as

$$\Delta P = \frac{Tu}{\eta_D} - P_e, \tag{1}$$

where T is wind propulsion system thrust, u is the vessel speed, η_D is the total propulsive efficiency and P_e is the electric consumption of the wind propulsion device. In the scaling phase, 0.7 was used for η_D value, but in the actual simulations, η_D varies with the propeller thrust magnitude.

The main engine equivalent power comparison for different wind propulsion devices is shown in figure 1. The performance models used to create this graph are presented in section 2.2.2. From this example, the basic difference in the thrust-generating properties of different wind propulsion devices can be seen. All the systems have the same area under the curve, but the wing sails and suction wings have better upwind performance whereas rotor sails perform better in beam and down winds.

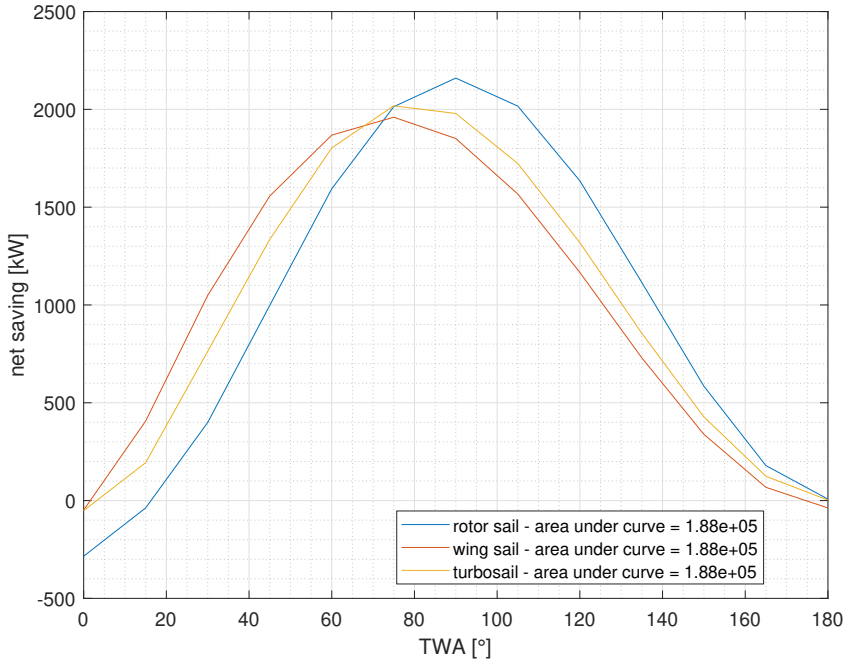

Figure 1. Main engine equivalent power for different systems at 13 kn vessel speed and 12.5 kn true wind speed.

2.1.2 Performance prediction

The hydrodynamic response of the ship was modeled using a Performance Prediction Program (PPP) developed by D-ICE. PPP calculates the brake power of the vessel by solving the surge, sway, yaw, and heel steady-equilibrium equations in a set of different prevailing conditions. More precisely, we calculate the brake power on predefined discrete values of vessel speed, wind speed and angle, and wave height and angle, leading to 5-dimensional matrices which can be used in the weather routing phase. Decoupling wave and wind allows us to model also cases where wave and wind direction are not the same. Based on the model decomposition and superposition principle, loads applying on the vessel are supposed independent and special dedicated interaction models are considered when interactions between models are required. Linearisations are considered around operational points for particular models (drift-added resistance requires hydrodynamic derivatives computed at the service speed, for example). The forces on the vessel were modeled using semi-empirical relations. For

calm water resistance we used Holtrop, 1984, and for propeller forces we used a regression model for Wageningen B-series propeller curves, Bernitsas M.M., 1981. We used Fuji, 1960 simplified model for rudder, and Mittendorf, M., U.D. Nielsen, H.B. Bingham, and S. Liu, 2022 relation for the wave-added resistance. Finally, we used Yasukawa, H., and Y. Yoshimura, 2015 relations for drift and added resistance and Fujiwara, 2005 relations for the wind loads on the hull and superstructures.

The sails loads and related active power are interpolated in 3D tables varying with Speed Through Water (STW), True Wind Speed (TWS), and True Wind Angle (TWA), pre-trimmed for maximum thrust. A depowering process is then applied to ensure that the 4 equilibrium equations can be solved under all environmental conditions. This process consists of a reducing coefficient multiplied on all load components, but not the active power. This coefficient is optimized based on a brake power minimization objective function, along with physical constraints (maximum rudder, leeway and roll angles, etc). The combination of these two approaches (interpolation in pre-trimmed tables and depowering) allow us, as a third party evaluating WASP performances, to consider data that wind propellers providers are open to share (i.e. pre-trimmed tables), on contrary to more confidential models and control heuristics.

2.1.3 Weather routing

The problem of optimizing ship routes is a complex problem due to the continuous nature of the ocean, the time-dependency of environmental fields, and the possible multiple objectives to optimize. Depending on the case of application, different variations of the problem occur, but methodologies are generally discrete. More precisely, the control variables (heading and brake power for example) considered in the problem often have predefined discrete values. We can distinguish three kinds of methodologies. First, fixed-grid approaches that are based on a predefined discretization of the search space, such as dynamic programming (Shao et al., 2012; Zaccone, R., E. Ottaviani, M. Figari, and M. Altosole, 2018) or graph-based shortest paths algorithms (Veneti et al., 2015; Chauveau et al., 2017; Wang et al., 2019). Second, dynamic-grid approaches that discover on-the-fly the search space during the algorithm, such as the isochrone (James, 1957; Hagiwara, 1989) and isopone (Klompstra et al., 1992) methods. Finally, evolutionary approaches start from an initial population of solutions and then, from mutations and crossover operations, explore other candidates. For a more complete survey of ship route optimization, see the work of Dupuy et al., 2020. The choice between these methods depends on the objective(s) to optimize, the constraints to satisfy, and the number of control variables.

In this work, we are studying multi-objective weather routing for wind-assisted ships and therefore we face some challenges because each of the previously introduced methods has its area of application. For example, dynamic-grid methods are more adapted to sailing ships, whose optimal routes are strongly impacted by the weather conditions, while fixed-grid methods are more adapted to merchant ships, which need to optimize multiple objectives and whose optimal routes stay around the direct one. D-ICE developed a graph-based approach to compute optimal paths for mono and multi-objective time-dependent shortest path problems with two control variables (ship heading and ship speed over ground). The impact of considering two control variables simultaneously is enhanced by wind assistance, as presented in Dupuy, M., D. Dudka, L. Letournel, F. Rongere, and G. Vincke, 2023.

As the ocean is a continuous space there is no straightforward way to mesh it. Various methods can be used for ocean meshing depending on the application (such as unstructured meshing for sailing ships) but in this work, we will use a distribution of positions perpendicularly away from the great circle route. Once the space is discretized, we expand the graph with parallel edges labelled with each discrete value of the second control value, the ship speed. Then, we apply on this graph a label-correcting multi-objective shortest path algorithm to compute Pareto optimal paths.

In this work, we consider a bi-dimensional cost function representing the travel time and the energy consumption in kWh.

2.1.4 Weather routing benefit

The fuel savings due to wind propulsion on a great circle route with constant speed is defined as the difference between the fuel consumption with and without a wind propulsion device.

$$\Delta F = F_{\mathrm{nosails|GCR-CS}} - F_{\mathrm{withsails|GCR-CS}}, \tag{2}$$

where F is the fuel consumption and ΔF is the fuel saving due to the wind propulsion system.

In this study, the weather routing benefit W_B was defined as a proportional increase in fuel savings when using the wind propulsion system together with the route and speed optimization compared to the great circle route with constant speed.

$$W_B = 100\left(\frac{F_{\mathrm{nosails|GCR-CS}} - F_{\mathrm{withsails|OR-OS}}}{\Delta F} - 1\right) \tag{3}$$

2.2 Input data

2.2.1 Ship model

The case study was carried out for a general Post-Panamax bulk carrier. The main characteristics of the vessel are shown in table 1.

Table 1. Vessel's main characteristics.

Characteristics		
Description	Value	Unit
Deadweight	75000	t
Lenght overall	230	m
Design draft	12	m
Ballast draft	6	m
Breadth	38	m
MCR	10 700	kW

2.2.2 Wind Propulsion Systems

Three different sail types were selected for the case study: rotor sails, flapped wing sails, and suction wings. The sail plans are shown in figure 2. No interaction between systems has been considered in the study.

For each system, the wind propulsion main engine equivalent power ΔP was optimized for different wind and wave conditions. The optimization variables vary from system to system, for rotor sails the only variable is rotor rpm and for suction wings and wing sails optimization, variables are the angle of attack, flap deflection β, and also suction speed u_s for suction wings. As a result of the optimization, force values, and power consumption were obtained in each wind condition producing force and power consumption matrices that were used in the voyage optimization.

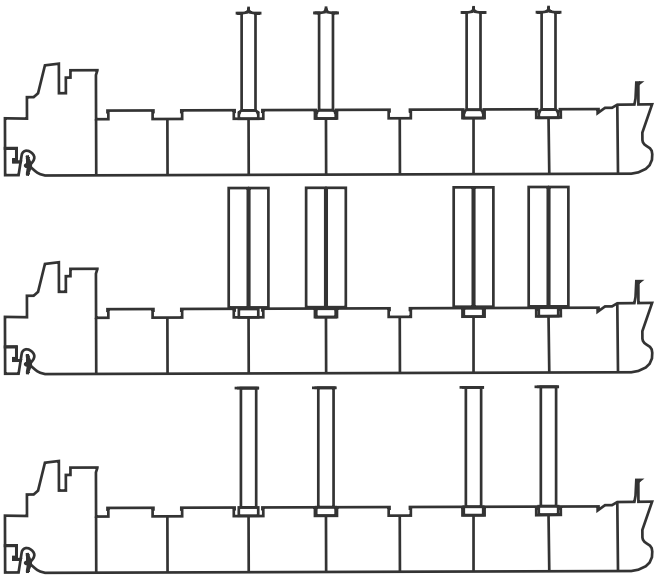

Figure 2. Studied sail plans for the Post Panamax bulk carrier. All the sails are located on the vessel's centerline. From top to bottom: rotor sails, flapped wing sails, and suction wings.

Rotor sails

A rotor sail is a rotating cylinder that utilizes the Magnus effect to produce lift force in suitable wind conditions. The lift and drag coefficients used for the rotor sails in this study were measured on board of RORO-vessel SC Connector equipped with two Norsepower 35 m x 5 m rotor sails. The ship was installed with a novel force measurement system and a state-of-the-art wind measurement system with 4 lidar beams to measure the lift and drag coefficients accurately in different wind conditions. The initial results of the measurement and analysis are shown in figure 3. The lift and drag coefficients are shown as a function of spin ratio which is defined as a ratio between rotor sail surface speed and apparent wind speed. The power consumption of the Norsepower rotor sails is also based on full-scale measurements.

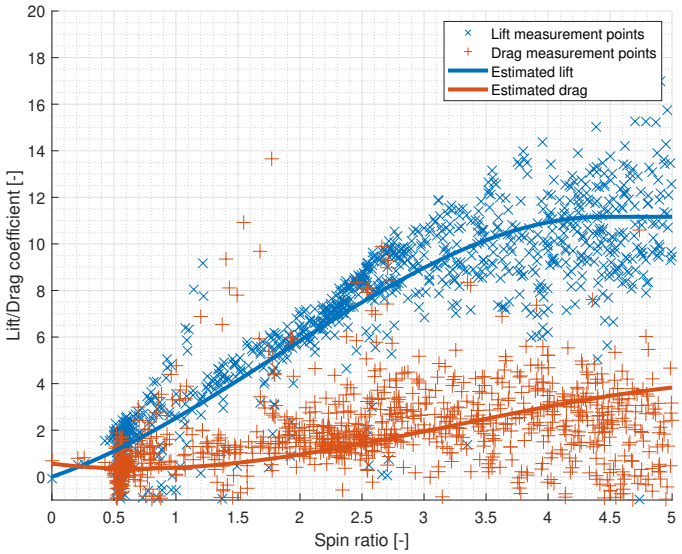

Figure 3. Norsepower rotor sail lift and drag measurement results and estimates as a function of spin ratio.

Wing sails

Wing sails are rigid wings that consist of a main element and flap. The flap angle β can be controlled separately to increase the camber of the sail enabling the wing to produce higher lift forces. The lift and drag coefficients of a wing sail with a flap used in this study were measured by Furukawa et al., 2015 in an open-return wind tunnel at the University of Auckland. The studied wing had the same chord length of 500 mm for the main element and the flap. Both elements had 64 pressure taps attached to the surface, measuring the pressure field around the wing. The lift and drag coefficients varying with angle of attack α with two different flap angles β are shown in figure 4.

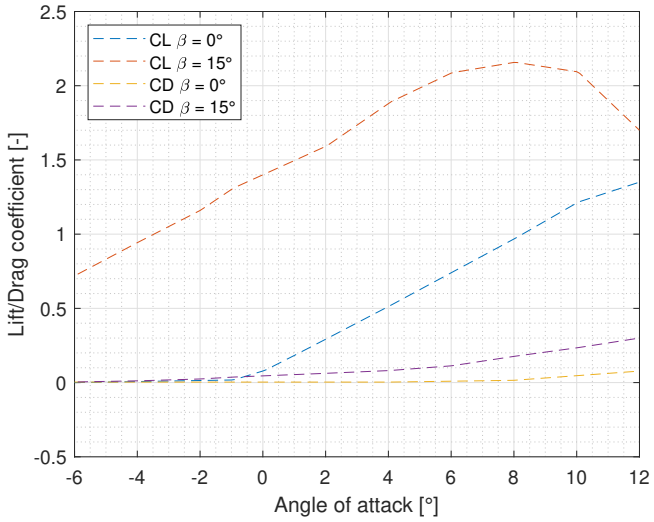

Figure 4. Lift and drag coefficients of a wing sail measured by Furukawa et al. (2015). In the original paper the data was missing for $\alpha < 0°$ with $\beta = 0°$, but CD was assumed to stay constant and CL was set to zero for computational reasons.

Wing sails are a passive wind propulsion system and they do not consume electricity in steady-state conditions, but to account for the trimming of the sail an average power consumption of 10 kW was considered.

Suction wings

The suction wing is a type of wing sail, but with a thicker main element providing higher lift-producing capability. To prevent the boundary layer from separating from the sail surface, the air is drawn inside the sail through a suction mesh. The lift and drag coefficients of the suction wing were taken from CFD simulations carried out by Hopes et al., 2021. The lift and drag curves are shown in figures 5 and 6 based on the sail's suction coefficient C_q defined by the equation :

$$C_q = \frac{Q}{U_i Z_m c} \tag{4}$$

where Q is the volumetric flow rate, U_i is the freestream velocity, Z_m the height and c the chord of the suction aerofoil. In the legends, Cq is suffixed with its values multiplied by 1000 ($Cq0023$ means $C_q = 0.023$).

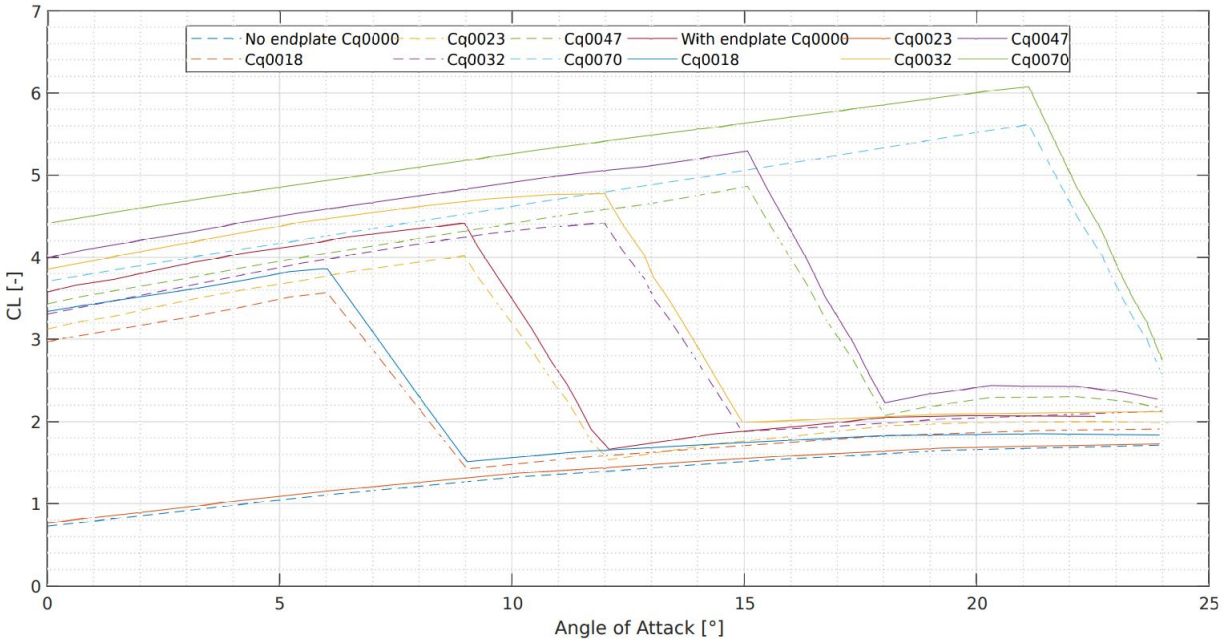

Figure 5. Lift curves of a suction wing with varying suction coefficient C_q.

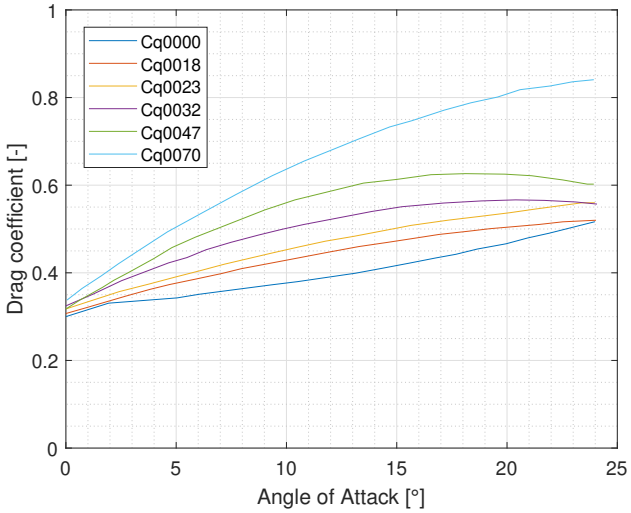

Figure 6. Drag curves of a suction wing with varying suction coefficient C_q.

The electric power consumption for the air suction P_e of the suction wings was estimated from the suction velocity u_s:

$$P_e = \frac{1}{\eta_e}\frac{1}{2}\rho A u_s^3, \tag{5}$$

where ρ is the air density, A is the cross-sectional area of the suction mesh and η_e is the electric efficiency including possible energy losses for which a value of 0.5 was used.

2.3 Environmental fields

We used the reanalysis dataset ERA5 from the European Center for Medium-Range Weather Forecast. From this dataset we get 10m components of wind, and also significant height, period, and direction for combined wind waves and swell. These reanalysis weather data, which are a merging between models and observations, should be close to the weather that really occurred.

For ocean currents, we used reanalysis dataset from Copernicus Marine Environmental Monitoring Service, generated from Mercator Ocean model NEMO 3.6. This dataset does not include tidal currents, but only geostrophic ones.

2.4 Route definition and constraints

We conducted this study on one of the biggest soybean shipping routes, mainly used by bulk carriers which goes from Brazil (Santos: 24.08 S, 46.32 W) to China (Qindgao: 35.96 N, 120.47 E), in both directions. The route passes through the strait of Malacca and we did not include any navigation restrictions.

The study covers a range of departure dates from 01.01.2015 to 01.01.2020 with a weekly frequency, and each computation included voyage duration constraint to respect a service speed of 13 knots (classic for the kind of ship considered).

3 RESULTS AND ANALYSIS

3.1 Route metocean analysis

The studied route passing through the southern ocean, we can expect to have important wind resources, and as there are few geographical constraints in the South Atlantic and Indian Ocean, we can expect to have important savings associated with wind propulsion and weather routing.

In Figure 7 are presented the distributions of wind and waves for the GCR-CS run. We have global wind coming from the east with important dispersion and a mean TWS of 12.5 kn. Waves are mainly coming from the southwest, with a mean H_S of 2 m.

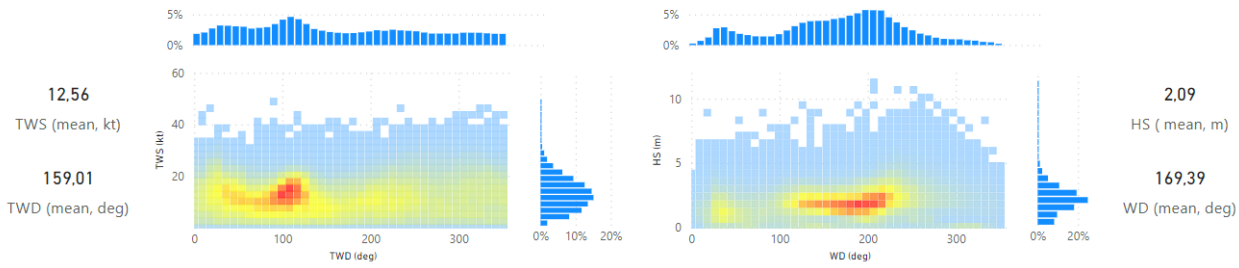

Figure 7. Metocean conditions on the studied route.

Regarding the projections of environmental conditions upon the ship axis in figure 8, we see that on the direct route, we have wind angles mainly from the [0 - 80] sector and waves from the [70 - 160] sector for the Santos to Qindgao direction, and the opposite in the other direction. We can therefore expect to have more savings associated with wind propulsion and weather routing in the direction Santos to Qindgao thanks to waves.

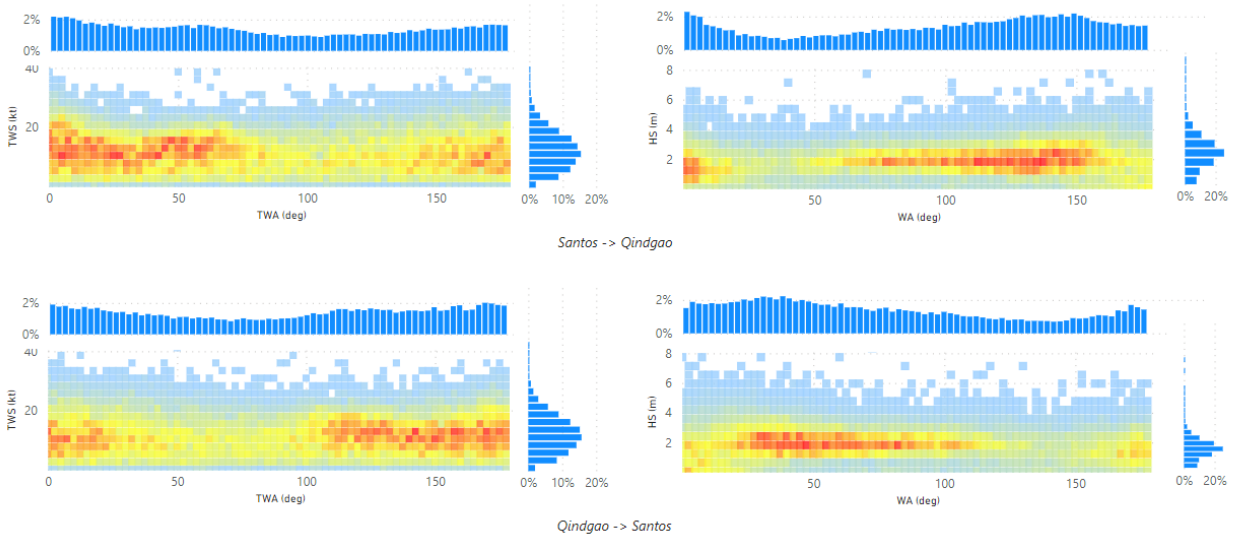

Figure 8. Metocean conditions on the ship axis.

An important specificity of this route is that wind direction and wave direction are de-correlated for a significant amount of time (40% of the time with a difference over 45 degrees). This enforce the importance of using a 5-dimensional polar table which de-corelate wind and waves conditions as explained in section 2.1.2.

3.2 System differences

3.2.1 Versatility vs specificity

An interesting observation in figure 1 is the shape of each curve. The net savings distribution peak width can be interpreted as a measure of system adaptability. We can sort these systems in terms of versatility: first the wing sails, then the suction wings, and finally the rotors sails. Besides, a consequence of the methods we applied to scale the systems is that the narrower the distribution peak, the greater the peak value (to have the same area below each curve). We can consider it as a measure of systems specificity. We have consequently the following order in terms of specificity: first the rotor, then the suction wing, and finally the wing sail.

3.2.2 Ships optimal operating points

From the polar table of each hybrid ship, which contains the evolution of required power (brake power + sails required power) to sail at a specific speed in various environmental conditions, we can evaluate the optimal operating points of the ship. As wind and waves have an important impact on hybrid ships' behavior, the optimal operating point is not only the wind angle that maximizes the sail's power. In figure 9 is presented the evolution of total power with TWA required to sail at different STW, in 15 knots of wind, without waves (solid line) or with 2 m of H_S aligned with the wind (dashed). It is interesting to see how considering waves shifts the optimal operating point (minimum of total power) to bigger TWA.

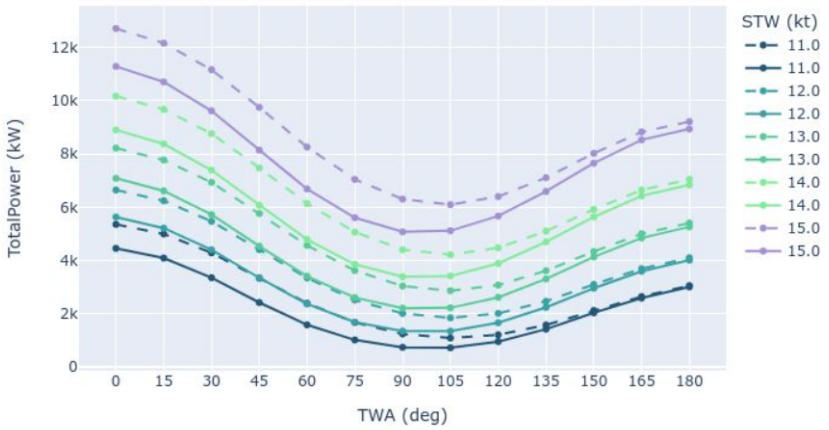

Figure 9. Evolution of hybrid ship total power with true wind angle (15 kn of TWS, H_S = 0 m (solid) and H_S = 2 m (dashed).

We also see in figure 10 the evolution of the optimal TWA (corresponding to minimum total power in figure 9) depending on discrete values of boat speeds for each wind propulsion system and we see that optimal TWA increases from the wing sails to the suction wings and finally to the rotor sails. This is a direct consequence of the lift and drag characteristics of the sail. Suction wings and wing sails are characterized by low drag coefficients giving better upwind performance. On the other hand, rotor sails have a greater lift-producing capability and larger drag giving them a better beam and downwind performance.

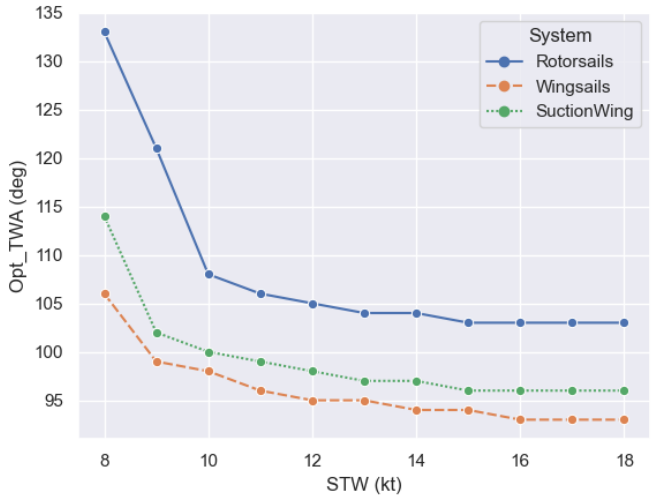

Figure 10. Evolution of optimal TWA depending on wind propulsion system (15 kn of TWS, H_S = 2 m).

3.2.3 Weather routing operating points

As presented in Dupuy, M., D. Dudka, L. Letournel, F. Rongere, and G. Vincke, 2023, the global strategy of the combined optimization of route and speed for wind-assisted ships is to accelerate or slow down whether the ship faces good or bad weather conditions and also to optimize the route to meet favorable environmental conditions. More precisely, considering the sensitivity to the wind of a hybrid vessel, the algorithm aims at finding routes with favorable true wind angles. Besides, the

optimization of route and speed simultaneously helps to act directly on the apparent wind angle. As an example, in figure 11 where colors represent occurrences in specific weather conditions, we see the differences between the GCR-CS and OR-OS scenario for the system Norsepower. We clearly see that the algorithm focuses on a specific range of TWA: for the direction Santos to Qingdao the mean value increases from 85° to 99° and the standard deviation decreases from 55° to 43°. We observe the same behavior in the other direction.

Figure 11. Wind statistics for the GCR-CS and OR-OS scenario, in both directions (Norsepower system).

In figure 12 are represented the occurrences of TWA in all OR-OS runs depending on the wind propulsion system. In this figure, we clearly see the same trend as in figure 1 and in the previous section, which confirms that the weather routing strategy takes benefits from the optimal operating points of each ship.

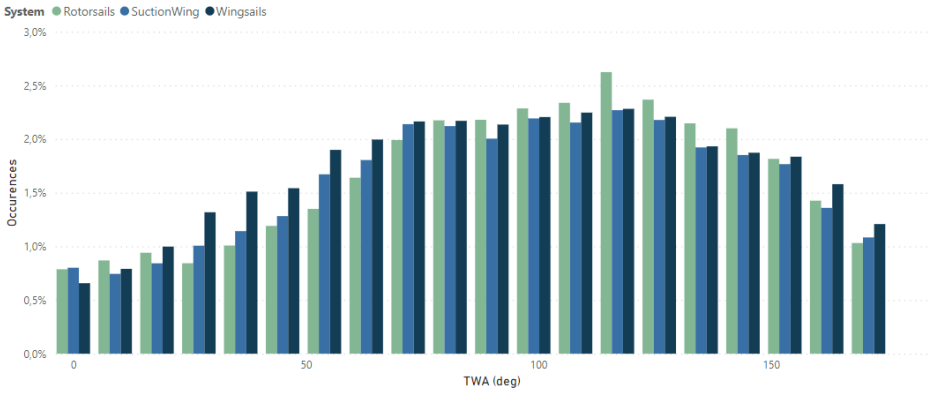

Figure 12. TWA repartition depending on the wind propulsion system in the OR-OS run.

In table 2 are presented the mean values of each environmental variable, depending on the routing scenario, the route, and the system. It is interesting to note that weather routing optimization manage to find angles consistent with TWA optimal values computed in section 3.2.2: in the Santos to Qingdao direction mean TWA increases from 86° to 97°-99.5° depending on the systems, and in the opposite direction from 94° to 98°-102°. Waves angles are also increased thanks to weather routing: from mean values of 101° to 115-117° in the Santos to Qingdao direction, and from 79° to 85-87° in the opposite direction.

We also see that due to the wave-added resistance which is higher for head waves than for following

waves, weather routing can find routes with higher wind speeds (around 15 kn vs 12.9 kn) and waves H_S (around 2.4 m vs 2 m) in the Santos to Qingdao direction than in the opposite.

Table 2. Mean environmental conditions depending on optimization scenario and systems.

Santos-Qingdao					
Scenario	System	TWA (deg)	W_A (deg)	TWS (kn)	H_S (m)
GCR-CS	Ref	86.05	100.89	12.57	2.09
OR-OS	Rotor	99.43	117.02	15.23	2.41
OR-OS	Suction	97.60	115.66	15.17	2.39
OR-OS	Wing	96.94	115.41	15.15	2.39

Qingdao-Santos					
Scenario	System	TWA (deg)	W_A (deg)	TWS (kn)	H_S (m)
GCR-CS	Ref	94.03	79.64	12.58	2.07
OR-OS	Rotor	102.37	87.02	12.96	2.03
OR-OS	Suction	99.80	86.24	12.93	2.03
OR-OS	Wing	98.12	85.09	12.99	2.03

3.3 Global results analysis

As explained in sect 2.1, from the comparison of GCR-CS scenario of the motor ship and hybrid ships, we get the shortest route saving. Then, comparing the GCR-CS run of the motor ship with the OR-OS run of hybrid ships, we get the optimized route savings. And finally, we get the weather routing benefit, meaning how weather routing enhances wind propulsion performances. It has to be reminded here that all the voyages are optimized to reduce consumption while keeping the voyage duration constant. In table 3 are presented these savings for each wind propulsion system and each route, as well as for the roundtrip.

Table 3. summary of the average results.

Santos-Qingdao			
	Shortest route saving	Optimized route saving	Weather routing benefit
Rotor sails	20.90%	46.15%	140.40%
Suction wings	23.33%	46.06%	106.05%
Wing sails	23.18%	46.02%	91.56%

Qingdao-Santos			
	Shortest route saving	Optimized route saving	Weather routing benefit
Rotor sails	21.18%	35.07%	69.39%
Suction wings	22.21%	34.64%	58.38%
Wing sails	21.29%	32.64%	55.09%

Roundtrip: Santos-Qingdao			
	Shortest route saving	Optimized route saving	Weather routing benefit
Rotor sails	21.04%	40.61%	104.89%
Suction wings	22.77%	40.35%	82.22%
Wing sails	22.23%	37.83%	73.33%

3.3.1 Wave influence

As presented in section 3.1, the route has mainly side / following waves in the Santos to Qingdao direction and side / head waves in the opposite direction. This is interesting to note that due to the large added resistance in waves for head waves (waves angle < 90°), and therefore larger ship consumption, optimizing the route which possibly increases the total traveled distance is harder. This explains the lower savings and lower weather routing benefits presented in the table 3 above. On the opposite, when the ship has mainly following waves (with small added wave resistance), the weather routing has more freedom to optimize the route.

3.3.2 Shortest route savings

First of all, we see that the scaling being based on a constant TWS of 12.5 knots (which is the mean TWS on the GCR-CS scenario), we do not have constant shortest route savings. This is a consequence of the aforementioned system differences in terms of versatility. We may indeed have a wide range of weather conditions in the GCR-CS scenario, which requires versatile wind propulsion devices. This drawback impacts especially the rotor sail on the Santos to Qingdao route, where we mainly have upwind conditions as presented in section 3.1. On the other direction, we have more comparable shortest route savings between sail technologies.

3.3.3 Optimized route savings

While analyzing optimized route savings, we see again another consequence of the versatility of each system mentioned above and our approach for scaling. As the weather routing strategy is to take benefit from this peak value, or more precisely from the optimal operating points presented before, we have the same trend for optimized route benefits as for the specificity mentioned in section 3.2.1: first the rotor, then the suction wing, and finally the wing sail.

However, a direct consequence is that the more specific a system is, the more complex it is to find a path sailing in these conditions, which may lead to longer paths. It is interesting to see in figure 13 the route travelled distances distribution depending on the wind propulsion system. Either in terms of mean values and distribution peak width, we have the same trend for travelled distance than for versatility: first the wing sails, then the suction wings, and finally the rotor sails. We also see in this figure that the travelled distance is more important in the Santos to Qingdao direction, which highlights that this route is more favorable for weather routing.

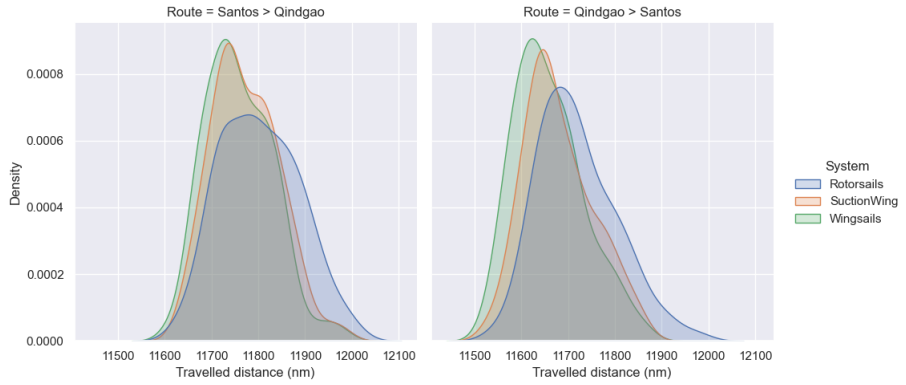

Figure 13. Evolution of route distance depending on wind propulsion system in the OR-OS run.

Weather routing benefits

The weather routing benefits presented here are impressive and specific to each technology. Again, the difference is a direct consequence of each system's versatility and our approach for scaling: while having a specific system is a disadvantage for the GCR-CS scenario, it is an advantage for OR-OS one. We, therefore, have greater weather routing benefits for the rotor sail, then for the suction wing, and finally for the wing sail.

4 LIMITS OF THE STUDY

This study compared the impact of weather routing on different hybrid vessels, equipped with 3 different sails technologies. While the rotor sail was based on the Norsepower system, the two other systems used generic models, which may have different performances than commercial systems. Even if we tried to be fair with our scaling methodology, we may have different conclusions from other sails models in terms of performance, but we hope the weather routing behavior would be the same. Another limitation is that we did not consider any interaction between sails, which impacts the performances of wind propulsion devices and can be different depending on the technology. While it may impact the percentages, we hope that it would not impact our conclusions about systems sensitivity to weather route optimization. Additionally, Norsepower performance data are issued from full-scale measurements with two rotors, while in this study we consider 4. Again, we think that the principal conclusions of this paper should not be impacted by this difference. Finally, in this study we used historical weather data, meaning that the optimization always chose the best path, knowing exactly the weather evolution. In operational routing, forecast uncertainties may lead to suboptimal choices and finally less global savings.

5 CONCLUSION

Weather routing benefits were examined on a Santos-Qingdao route for a post-Panamax bulk carrier equipped with different wind propulsion systems. The studied wind propulsion systems included rotor sails, suction wings, and wing sails and there were differences in how much the different wind propulsion systems can benefit from voyage optimization. The systems were scaled in order to have the same baseline performances on the route mean weather conditions. With the analysis of a large set of voyages (5 years with a weekly departure), we showed that the weather routing optimization strategy is to take benefits from ship optimal operating points which varies with sail technologies: while wing sail and suction wings have better upwind performance, rotors have greater beam and downwind performance. Besides, from the comparison between different routing scenario, we showed that while versatility of a sail is an advantage for shortest route savings, sails specificity enhances optimized route savings and consequently the traveled distance. The average weather routing benefit with wing sails was 73.33%, 82.22% with suction wings, and 104.89% with rotor sails. In this paper, the weather routing benefit was studied for a single route, but the authors believe that the results will hold qualitatively for more general cases as well.

REFERENCES

Bernitsas M.M. Ray D., Kinley P. (1981). "KT, KQ, and Efficiency Curves for the Wageningen B-series Propellers". In: *Deparmtent of Naval Architecture and Marine Engineering, College of Engineering, The University of Michigan*.

Chauveau, E., P. Jegou, and N. Prcovic (2017). "Weather Routing Optimization: A New Shortest Path Algorithm". en. In: *2017 IEEE 29th International Conference on Tools with Artificial Intelligence (ICTAI)*. Boston, MA: IEEE, pp. 687–694. ISBN: 978-1-5386-3876-7. DOI: 10.1109/ICTAI.2017.00110. URL: https://ieeexplore.ieee.org/document/8372013/.

Dupuy, M., C. D'Ambrosio, and L. Liberti (2020). "Optimal Paths on the Ocean". In: *Encyclopedia of Optimization*. Ed. by P. M. Pardalos and O. A. Prokopyev. Cham: Springer International Publishing, pp. 1–10. ISBN: 978-3-030-54621-2. DOI: 10.1007/978-3-030-54621-2_745-1. URL: https://doi.org/10.1007/978-3-030-54621-2_745-1.

Dupuy, M., D. Dudka, L. Letournel, F. Rongere, and G. Vincke (2023). "About the Benefit of Optimizing both Speed and Route in Wind-Assisted Ships Multi-Objective Weather Routing". In: *RINA Wind Propulsion Conference 2023*.

Fuji, H. (1960). "Experimental Researches on Rudder Performance". In: *J. Zosen Kiokai 107, 105-111,*

Fujiwara, T. (2005). "A New Estimation Method of Wind Forces and Moments Acting on Ships on the Basis of Physical Component Models". In: *Journal of the Japan society of naval architects and ocean engineers, 2, 243–255*.

Furukawa, Hiroyuki et al. (2015). "Performance of wing sail with multi element by two-dimensional wind tunnel investigations". In: *Journal of Fluid Science and Technology* 10, JFST0019–JFST0019. DOI: 10.1299/jfst.2015jfst0019.

Hagiwara, H. (1989). "Weather Routing of (Sail-Assisted) Motor Vessels". PhD thesis. Delft: Delft University of Technology.

Holtrop, J. (1984). "A Statistical Re-Analysis of Resistance and Propulsion Data". In: *International Shipbuilding Progress, ISP,Volume 31, Number 363*.

Hopes, W., D. Pearson, and J. Buckingham (Sept. 2021). "A CFD Study on Wind Assisted Propulsion Technology for Commercial Shipping". In: *RINA Wind Propulsion Conference 2021*.

James, R. W. (1957). *Application of Wave Forecasts to Marine Navigation*. Tech. rep. Washington, D.C.: U.S. Naval Oceanographic Office.

Klompstra, M. B., G. J. Olsder, and P. K. G. M. van Brunschot (1992). "The Isopone Method in Optimal Control". en. In: *Dynamics and Control* 2.3, pp. 281–301. ISSN: 1573-8450. DOI: 10.1007/BF02169518. URL: https://doi.org/10.1007/BF02169518.

Mason, J.C. (2021). "Quantifying Voyage Optimisation with Wind-Assisted Ship Propulsion: a New Climate Mitigation Strategy for Shipping". In: *Doctoral dissertation, The University of Manchester, (UK)*.

Mittendorf, M., U.D. Nielsen, H.B. Bingham, and S. Liu (2022). "Towards the Uncertainty Quantification of Semi-Empirical Formulas Applied to the Added Resistance of Ships in Waves of Arbitrary Heading". In: *Ocean Engineering, 251, 111040*.

Paakkari, V., H. Wang, and Stigler C. (2022). "Voyage Optimization with Wind Propulsion". In: *RINA ICCAS 2022*.

Sarsila, S. (2022). "Comparison of Achieved Fuel Savings on Ships by Different Wind Propulsion Devices using a 3-DoF Resistance Model". English. Master's thesis. Aalto University. School of Engineering, p. 43. URL: http://urn.fi/URN:NBN:fi:aalto-202205223282.

Shao, W., P. Zhou, and S. K. Thong (2012). "Development of a Novel Forward Dynamic Programming Method for Weather Routing". en. In: *Journal of Marine Science and Technology* 17.2, pp. 239–251. ISSN: 0948-4280, 1437-8213. DOI: 10.1007/s00773-011-0152-z.

Veneti, A., C. Konstantopoulos, and G. Pantziou (2015). “Continuous and Discrete Time Label Setting Algorithms for the Time Dependent Bi-Criteria Shortest Path Problem”. en. In: *INFORMS Computing Society Conference*. Ed. by Brian Borchers, J. Paul Brooks, and Laura McLay. Richmond, Virginia, pp. 62–73. ISBN: 978-0-9843378-6-6. DOI: 10.1287/ics.2015.0005. URL: https://www.informs.org/Find-Research-Publications/Multimedia-Books/ICS-Proceedings/2015-Conference-Volume/ICS-2015-Table-of-Contents.

Wang, H., W. Mao, and L. Eriksson (2019). “A Three-Dimensional Dijkstra’s Algorithm for Multi-Objective Ship Voyage Optimization”. en. In: *Ocean Engineering*. ISSN: 0029-8018. DOI: 10.1016/j.oceaneng.2019.106131. URL: http://www.sciencedirect.com/science/article/pii/S0029801819303208.

Yasukawa, H., and Y. Yoshimura (2015). “Introduction of MMG Standard Method for Ship Maneuvering Predictions”. In: *Journal of Marine Science and Technology, 37–52*.

Zaccone, R., E. Ottaviani, M. Figari, and M. Altosole (2018). “Ship Voyage Optimization for Safe and Energy-Efficient Navigation: A Dynamic Programming Approach”. en. In: *Ocean Engineering* 153, pp. 215–224. ISSN: 0029-8018. DOI: 10.1016/j.oceaneng.2018.01.100. URL: https://www.sciencedirect.com/science/article/pii/S0029801818301082.